24. S. T. Massie *et al*., *J. Geophys. Res.* **101**, 9757 (1996).
25. S. Sherwood, data not shown.
26. H. Pruppacher, J. D. Klett, *Microphysics of Clouds and Precipitation* (Kluwer, Dordrecht, Netherlands, ed. 2, 1997).
27. W. Ji, P. K. Wang, *J. Atmos. Sci.* **56**, 829 (1999).
28. The linearity assumption follows by noting from Fig. 1 that there was no apparent lag between variations in D_e and RH, and that the dehydration rate below 450 K was roughly proportional to q. The former circumstance implies a quasi-steady balance between sources and sinks of q near the tropopause, whereas the latter implies that the sinks (thus sources) must be proportional to q.
29. V. T. J. Phillips, T. W. Choularton, A. M. Blyth, J. Latham, *Q. J. R. Meteorol. Soc.*, in press.
30. R. A. Houghton, in *Global Biomass Burning*, J. S. Levine, Ed. (MIT Press, Cambridge, MA, 1991), pp. 321–325.
31. D. Rosenfeld, *Science* **287**, 1793 (2000).
32. C. Moulin, C. E. Lambert, F. Dulac, U. Dayan, *Nature* **387**, 691 (1997).
33. C. S. Bretherton, M. Widmann, V. P. Dymnikov, J. M. Wallace, I. Bladé, *J. Clim.* **12**, 1990 (1999).
34. G. H. Orcutt, S. F. James, *Biometrika* **35**, 397 (1948).
35. M. S. Bartlett, *J. R. Stat. Soc.* **98**, 536 (1935).
36. The number 20 was obtained by visually estimating the number of independent fluctuations in the data and subtracting 1. Computations using two common formulas based on autocovariance models (*33*) valid for general (*34*) and red-noise (*35*) processes yielded 18 and 37 degrees of freedom, respectively. All of these estimates are high enough to yield strongly significant results.
37. I thank A. Dessler for generously supplying key interpolated data sets, K. Rosenlof for providing vertical velocity calculations, A. Heymsfield for useful advice, and H. Zeleznik for editorial assistance. The ISCCP AVHRR data were obtained from the NASA Langley Atmospheric Sciences Data Center. Supported by NASA Earth Observing System Interdisciplinary Science program grant UPN 291-01-91.

6 August 2001; accepted 9 January 2002

Warming of the Southern Ocean Since the 1950s

Sarah T. Gille

Autonomous Lagrangian Circulation Explorer floats recorded temperatures in depths between 700 and 1100 meters in the Southern Ocean throughout the 1990s. These temperature records are systematically warmer than earlier hydrographic temperature measurements from the region, suggesting that mid-depth Southern Ocean temperatures have risen 0.17°C between the 1950s and the 1980s. This warming is faster than that of the global ocean and is concentrated within the Antarctic Circumpolar Current, where temperature rates of change are comparable to Southern Ocean atmospheric temperature increases.

The Southern Ocean plays a critical role in global climate. With no continental barriers, it serves as a conduit to transmit climatic signals between the Pacific, Atlantic, and Indian Oceans. The predominant current of the Southern Ocean, the fast-flowing Antarctic Circumpolar Current (ACC), is characterized by strongly tilting isopycnals. Because water mixes preferentially along constant density surfaces, tilting isopycnals bring mid-depth water into contact with the ocean surface and serve as a barrier to southward transport, possibly helping to isolate the Antarctic continent from mid-latitude climate variability (*1*).

Recent examinations of global ocean temperature changes have shown substantial warming in the upper 1000 m, averaging about 0.1°C between 1955 and 1995 (*2*). Southern Hemisphere ocean warming also averages about 0.1°C over the same time period, but detailed study of the Southern Ocean has been hampered by the limited number of shipboard observations available south of 30°S (*3*–*5*). This study makes use of the large number of mid-depth temperature observations collected during the 1990s by Autonomous Lagrangian Circulation Explorer (ALACE) floats to characterize modern-day temperatures in the Southern Ocean and compares these temperature measurements with historic shipboard measurements.

ALACE floats were deployed from research ships throughout the 1990s as part of the World Ocean Circulation Experiment (WOCE). The floats sink to a predetermined pressure and follow mid-depth ocean currents for a fixed time interval of 10 to 25 days. They then rise to the surface and relay their positions and the mean temperatures recorded at depth to the Argos communications satellite system (*6*). (Newer floats also measure vertical temperature profiles as they rise to the surface; because only a fraction of the 1990s ALACE floats did this, no float profile data was included in this analysis.) A typical float provided about 50 cycles of data over 2.5 years for this study; many of the floats continue to gather data today. In the region of the world's ocean south of 30°S between 700 and 1100 m depth, 12,659 mean temperature observations were collected between 1990 and 2000 (*7*). Because the floats drift with the ocean currents, the geographic distribution of data spans the entire Southern Ocean, as indicated in Fig. 1A. ALACE observations have been used to study global and regional ocean circulation in a variety of ways (*8*–*10*), but have not previously been used to study long-term climatic variability in the ocean.

Thermistors on ALACE floats are calibrated with an accuracy of 0.001° to 0.003°C, and the sensor calibration is expected to degrade by less than 0.001°C per year. Numerical truncation required to transmit temperatures via satellite (*11*) effectively adds noise but no bias to the data, and this noise is small compared with small-scale ocean variability. Salinities were not routinely measured by ALACE floats, so compensating changes in temperature and salinity cannot be examined using these observations.

ALACE temperature observations were compared with temperature profiles collected from research ships since the 1930s. In that time period, techniques used by ships to collect ocean temperatures have evolved substantially. Before the 1970s, temperatures were derived from pressure-protected reversing thermometers, which were accurate to 0.02°C (*12*). More recent observations are from electronic conductivity-temperature-depth (CTD) and expendable bathythermograph (XBT) sensors, with accuracies of 0.001°C and 0.05°C (*13*), respectively. There are no known biases between different temperature measurement techniques. Shipboard temperatures were drawn from two separate data archives. The first, the Southern Ocean Database (SODB), includes approximately 17,724 profiles from reversing thermometer and CTD data collected between 1930 and 1990 and between 70° and 30°S (*14*). The second, the World Ocean Database 1998 (WODB), gathers a total of 35,102 Southern Ocean temperature profiles from reversing thermometer, CTD, and XBT data that extend deeper than 700 m (*15*, *16*). Both data sets are archived at standard depths, approximately every 100 m in the depth range considered here (*17*). The databases were merged, and duplicate stations that appeared in both were removed.

For this study, ALACE temperature observations were paired with geographically nearby temperature profiles. In total, 439,851 ALACE/temperature profile pairs were within 220 km of each other, and 112,103 were within 110 km. Figure 1B shows the distribution of stations used in this study as a function of decade. Temperature profile data were then linearly interpolated to match the depth of the ALACE observations. All pairs of float and hydrography point measurements

Scripps Institution of Oceanography and Department of Mechanical and Aerospace Engineering, University of California San Diego, La Jolla, CA 92093–0230, USA. E-mail: sgille@ucsd.edu

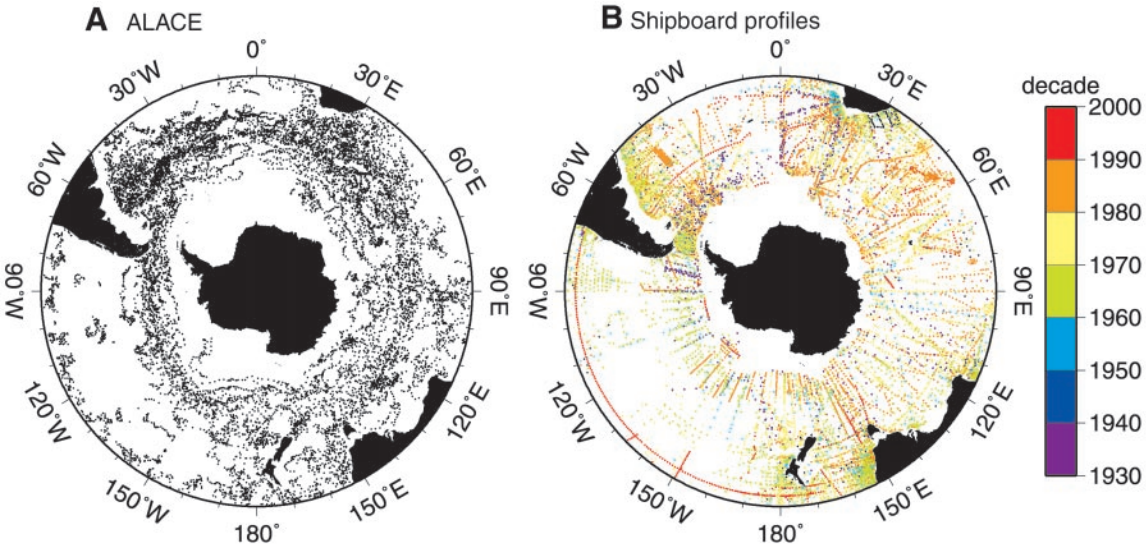

Fig. 1. (**A**) Distribution of the 12,437 ALACE temperature observations used in this study. Data were collected between 1990 and 2000 and are from 700 to 1100 m depth. Only ALACE measurements that were within 220 km of shipboard temperature profiles were retained for this analysis. (**B**) Distribution of shipboard temperature profiles used in this study as a function of decade. Bottle data, CTD data, and some XBT observations are included in these records. For this analysis a total of 20,659 stations from the WODB 98 and from the SODB were used. The northern boundary in both panels is at 30°S.

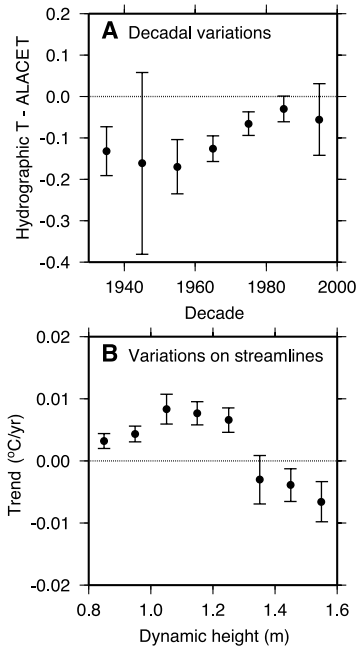

Fig. 2. (**A**) Difference between temperature profiles from shipboard observations and ALACE temperatures as a function of decade. To generate this figure, differences between ALACE temperatures and shipboard observations were bin-averaged on the basis of the decade when shipboard data were collected. Error bars are large in the 1990s, because many 1990s hydrographic observations have not yet entered the world ocean databases. (**B**) Temperature change per year as a function of dynamic height contour. Trends were computed from differences between hydrography and ALACE and then were bin-averaged on the basis of dynamic height. Thus, each point represents the mean anomaly for a 0.1 dynamic meter bin. Here, differences were computed from data points separated by less than 110 km in space. Dynamic heights of 1.2 m have an average latitude of 45.0°S; 1.0 m averages 52.5°S; 0.8 m averages 54.0°S (*32*).

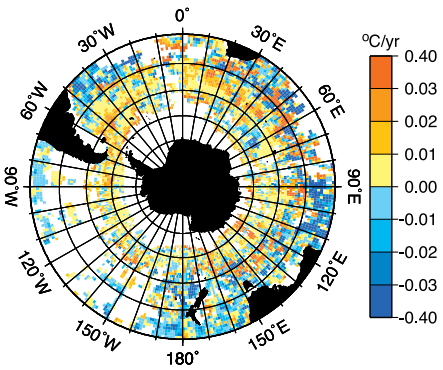

Fig. 3. Temperature trends computed from ALACE/hydrography differences bin-averaged in 1° by 1° squares. For this analysis, ALACE/hydrography pairs were used if the hydrographic measurements were collected after 1930, and they were separated from the ALACE observations by at least 10 years in time and by less than 220 km in space. Latitude and longitude grid lines are at 10° intervals.

between 700 and 1100 m depth are grouped together in this analysis.

Overall, for measurements within 220 km of each other in the region south of 35°S, ALACE temperatures were systematically 0.09° ± 0.02°C warmer than pre-1990 temperature profile data (*18*). Results computed using only SODB data or only WODB were not statistically different from results based on the composite data set, and only the composite data set results will be discussed here.

Because of high winds, high sea state, and lack of sunlight in the wintertime Southern Ocean, only 16% of shipboard observations south of 30°S and only 11% of shipboard observations south of 45°S were collected during the months of May, June, and July. In contrast, ALACE floats sample uniformly throughout the year, with 27% of observations from May through July. Because temperature biases could be caused by seasonal differences in the analysis period, the analysis was repeated using only observations obtained between October and March. Within error bars, long-term temperature variability was unchanged by this strategy and the remaining results reflect the full year-round observations.

Figure 2 sorts mean temperature differences between hydrographic profiles and 1990s ALACE temperatures as a function of decade in the latitude range from 35° to 65°S. Within error bars, data from the 1990s do not differ from ALACE observations, indicating that there is no measurable temperature bias in the ALACE observations. No detectable warming occurred between the 1930s and the 1950s, and few observations were collected during the 1940s, resulting in large error bars and no clear temperature signal. Warming is most rapid in the 1950s and 1960s and levels off in the 1980s and 1990s, in agreement with Southern Hemisphere trends reported elsewhere (*2*). However, the 0.17° ± 0.06°C warming seen in the 700 to 1100 m depth range of the Southern Ocean after 1950 is nearly double the global trend for the upper 1000 m of the ocean (*2*). This implies that the mid-depth Southern Ocean has heated more rapidly than the global ocean as a whole.

Averaging the temperature change per year for each pair of observations separated by less than 220 km produces a mean warming rate of 0.004° ± 0.001°C/year between 35° and 65°S. (For the trend calculations in this paper, hydrography from 1930 to 1989 was used, and a minimum of 10 years was required between float and hydrographic measurements.) Most of this warming occurs

between 45° and 60°S, in the latitude range of the ACC. Figure 3 shows temperature trends as a function of position. Overall patterns indicate cooling in the northern part of the domain and warming south of about 45°S.

Flow in the Southern Ocean is not strictly eastward; it follows the meandering path of the ACC, which is furthest north in the Atlantic and furthest south in the eastern Pacific. Figure 2B shows temperature change as a function of dynamic height contour. Here, dynamic height at 900 m depth has been computed from gridded atlas data (*19*) referenced to 3500 m depth. The core of the Subantarctic Front, the fast-moving northern jet of the ACC, coincides with steep gradients in dynamic height, located near 1.1 to 1.2 m dynamic height. Measurable warming has occurred between the 0.8 and 1.3 m dynamic height contours, and the most rapid warming is within the Subantarctic Front. In the jet core, warming averages 0.008° ± 0.002°C/year. This mid-depth ocean warming is slightly smaller than the mean atmospheric trend in the region, but it matches the atmospheric changes within error bars: Between 1949 and 1996, atmospheric warming rates averaged 0.013° ± 0.006°C/year at meteorological stations located on land in the Southern Ocean and 0.012° ± 0.007°C/year for stations on the Antarctic continent (*20*, *21*). Ocean warming error bars are smaller than the error bars of the land-based observations because the ocean observations provide a larger number of statistically independent observations than the land stations.

Figures 2B and 3 both show that the northern part of the Southern Ocean (north of the 1.3 m dynamic height contour) has cooled slightly, though the trend is not as pronounced as the warming further south. This cooling might be explained by reduced downwelling associated with a long-term drop in wind stress curl seen in National Centers for Environmental Prediction reanalysis winds south of 30°S (*22*); however, because of the limitations in Southern Hemisphere observations, reanalysis winds are not adequate for evaluating long-term trends south of 45°S (*23*, *24*) and could be questionable in the northern part of the Southern Ocean as well.

Because the warming found in this study is concentrated along the Subantarctic Front, it may be linked to Subantarctic Mode Water, which is ventilated annually and, therefore, responds rapidly to atmospheric changes (*25*–*27*). ALACE observations are point measurements and do not include salinity; therefore, they cannot be used to distinguish warming associated with temperature increases on a constant density surface (due to heating of Mode Water, for example) from warming due to displacement of water masses (*28*, *29*). Separate analysis of WOCE hydrographic sections suggests that both processes have occurred. Compared with earlier gridded hydrographic data (*14*), hydrographic lines show temperature changes that are consistent with a southward migration of the ACC over time of about 50 km in the Pacific (*30*) as well as the Atlantic and Indian Oceans (*31*). Warming at 700 to 1100 m depth slightly exceeds what would be expected merely from southward migration of isopycnals, suggesting that temperatures on isopycnals have increased. Overall, this implies a net warming and reduction in the volume of cold circumpolar waters that separate the ACC from the Antarctic continent. Such changes could potentially influence the volume and stability of Antarctic sea ice.

These observational results clearly indicate that the subsurface Southern Ocean has warmed during the past 50 years. These changes may have broader implications as the water that is ventilated in the region around Antarctica spreads gradually around the globe. The reduced volume of cold water and the increased temperatures of the latter half of the 20th century are likely to manifest themselves throughout the world's oceans in the decades to come, and they may be used as markers to help identify rates of mid-depth and deep ocean circulation and of global ocean heat storage. In addition, because warm water can hold less dissolved gas than cold water, the observed warming indicates that the CO_2 storage capacity of the Southern Ocean has decreased since the 1950s, and this may also have implications for global climate.

References and Notes

1. S. R. Rintoul, C. W. Hughes, D. Olbers, in *Ocean Circulation and Climate*, G. Siedler, J. Church, J. Gould, Eds. (Academic Press, San Diego, 2001), pp. 271–302.
2. S. Levitus, J. L. Antonov, T. P. Boyer, C. Stephens, *Science* **287**, 2225 (2000); see also its accompanying supplemental material, available on *Science* Online at www.sciencemag.org/feature/data/1046907.shl.
3. T. P. Boyer *et al.*, *World Ocean Database 1998*, vol. 5, *Temporal Distribution of Ocean Station Data Temperature Profiles*, NOAA Atlas NESDIS 22, (U.S. Government Printing Office, Washington, DC, 1998).
4. P. S. Wong, N. L. Bindoff, J. A. Church, *J. Clim.* **14**, 1613 (2001).
5. T. P. Barnett, D. W. Pierce, R. Schnur, *Science* **292**, 270 (2001).
6. R. E. Davis, D. C. Webb, L. A. Regier, J. Dufour, *J. Atmos. Ocean. Tech.* **9**, 264 (1992).
7. ALACE data used in this study are available at the Web site for the WOCE Float Data Assembly Center, http://wfdac.whoi.edu/.
8. R. E. Davis, P. D. Killworth, J. R. Blundell, *J. Geophys. Res.* **101**, 855 (1996).
9. R. E. Davis, *J. Geophys. Res.* **103**, 24,619 (1998).
10. K. L. Lavender, R. E. Davis, W. B. Owens, *Nature* **407**, 66 (2000).
11. R. E. Davis, personal communication (2001).
12. W. Mantyla, thesis, University of California, San Diego (1970).
13. D. Roemmich, B. Cornuelle, *Deep-Sea Res.* **34**, 299 (1987).
14. D. Olbers, V. Gouretski, G. Seiss, J. Schröter, *Hydrographic Atlas of the Southern Ocean*, (Alfred Wegener Institute, Bremerhaven, Germany, 1992).
15. S. Levitus *et al.*, *World Ocean Database 1998*, vol. 1, *Introduction. NOAA Atlas NESDIS 18* (U.S. Government Printing Office, Washington, DC, 1998).
16. M. E. Conkright *et al.*, *World Ocean Database 1998* (CD-ROM data set), *National Oceanographic Data Center Report 14*, (NODC, Silver Spring, MD, 1998).
17. WODB is also archived at the depths reported by the original investigators. The original data are not as extensively quality controlled as the standard depth data and were therefore not used in this study.
18. Error bars of mean values reported in this paper represent 2σ errors. They are computed by doubling the standard deviation and dividing by the square root of the number of degrees of freedom. Because ALACE temperatures can be paired with more than one shipboard profile (and vice versa), in these calculations the number of degrees of freedom is $2N_1 N_2/(N_1+N_2)$ where N_1 and N_2 are the number of independent temperature observations from floats and profiles that have been used to compute mean temperature differences or warming trends, respectively.
19. V. V. Gouretski, K. Jancke, *WHP SAC Tech. Rep. No. 3, WOCE Report No. 162/98*, (WOCE Special Analysis Centre, Max-Planck Institute, Hamburg, 1998).
20. T. H. Jacka, W. F. Budd, *Ann. Glaciol.* **27**, 553 (1998).
21. Fifteen Southern Ocean and seven Pacific Island stations are combined in (*20*). Southern Ocean trends are computed by omitting the data from Roratonga, Tahiti, Rapa, Pitcairn Island, Easter Island, and Juan Fernandez from the database. Error bars are two times the standard deviation divided by $\sqrt{N}$, where N is 15 for the Southern Ocean and 16 for the Antarctic continent.
22. E. Kalnay *et al.*, *Bull. Am. Meteorol. Soc.* **77**, 437 (1996).
23. K. M. Hines, D. H. Bromwich, G. J. Marshall *J. Clim.* **13**, 3940 (2000).
24. R. Kistler *et al.*, *Bull. Am. Meteorol. Soc.* **82**, 247 (2001).
25. M. S. McCartney, in *A Voyage of Discovery, George Deacon 70th Anniversary Volume*, M. Angel, Ed. (Pergamon, Oxford, 1977), pp. 103–119.
26. M. S. McCartney, *J. Mar. Res.* **40**, 427 (1982).
27. K. Hanawa, L. D. Talley, in *Ocean Circulation and Climate*, G. Siedler, J. Church, J. Gould, Eds. (Academic Press, San Diego, 2001), pp. 373–386.
28. S. Levitus, *J. Geophys. Res.* **94**, 6091 (1989).
29. N. Bindoff, T. McDougall, *J. Phys. Oceanogr.* **24**, 1137 (1994).
30. J. H. Swift, *International WOCE Newsletter* **18**, 15 (1995), available at www.soc.soton.ac.uk/OTHERS/woceipo/publications/index.html.
31. Following the method in (*29*) but instead looking at displacements in the meridional direction rather than the vertical direction, warming at a fixed location can be partially interpreted as meridional migration of isopycnals, where $\Delta y_\sigma = \Delta\sigma/(\partial\sigma/\partial y)$. Here, $\Delta\sigma$ was computed as the difference between atlas density (*14*) and density from the Southern Ocean WOCE sections (A12, A16, A21, I06, I08, P11, P14, P16, P17, and P18), whereas meridional density gradients $\partial\sigma/\partial y$ were computed from atlas data alone. At depths of 700, 800, 900, 1000, and 1100 m in regions where density increased toward the poles by at least 0.02 kg m^{-3} per degree latitude, Δy_σ ranged from 50 to 70 km southward. In the vocabulary used in (*29*), this isopycnal shift is "pure heave," and the associated temperature change represents the maximum warming that can be explained by isopycnal displacement alone. Even if density does not change, temperature can increase if it is compensated by an increase in salinity. In a noise-free ocean, the salinity-compensated warming would appear as a meridional migration of isotherms that differed from the migration of isopycnals, giving $\Delta y_\theta = \Delta\theta/(\partial\theta/\partial y) - \Delta y_\sigma$. For the WOCE sections, isotherms appear to migrate 8 to 12 km further south than isopycnals, implying that some compensated warming has occurred.
32. The mapped dynamic topography used for this analysis is available on *Science* Online at www.sciencemag.org/cgi/content/full/295/5558/1275/DC1.

33. R. Davis generously made the Southern Ocean ALACE data available for this study. Comments from R. Davis, V. Gouretski, L. Talley, A. Mantyla, W. Munk, J. Reid, D. Roemmich, and J. Swift helped with the analysis and interpretation of these results. This work was supported by the National Science Foundation under grant OCE-9985203/OCE-0049066.

30 August 2001; accepted 14 January 2002